JOURNAL OF AGRICULTURAL AND FOOD CHEMISTRY

Article

pubs.acs.org/JAFC

Metabolic Pathways of T-2 Toxin in in Vivo and in Vitro Systems of Wistar Rats

Shupeng Yang,[†,§,∥] Yanshen Li,[†,§,∥] Xingyuan Cao,[†,§] Dingfei Hu,[#] Zhanhui Wang,[†,§] Ying Wang,[†,§] Jianzhong Shen,[†,§] and Suxia Zhang*[,†,§]

[†]Department of Veterinary Pharmacology and Toxicology, College of Veterinary Medicine, China Agricultural University, Beijing 100193, People's Republic of China

[§]Key Laboratory of Detection for Veterinary Drug Residue and Illegal Additive, Ministry of Agriculture, People's Republic of China

[#]Department of Civil and Environmental Engineering, The University of Iowa, Iowa City, Iowa 52242, United States

ABSTRACT: In the present study, metabolites of T-2 toxin in in vivo and in vitro systems of Wistar rats were identified and elucidated by ultraperformance liquid chromatography−quadrupole/time-of-flight tandem mass spectrometry (UPLC-Q/TOF-MS). Expected and unexpected metabolites were detected by Metabolynx[XS] software, which could automatically compare MS[E] data from the sample and control. A total of 19 metabolites of T-2 toxin were identified in this research, 9 of them being novel, which were 15-deacetyl-T-2, 3′-OH-15-deacetyl-T-2, 3′,7-dihydroxy-T-2, isomer of 3′,7-dihydroxy-T-2, 7-OH-HT-2, isomer of 7-OH-HT-2, de-epoxy-3′,7-dihydroxy-HT-2, 9-OH-T-2, and 3′,9-dihydroxy-T-2. The results showed that the main metabolic pathways of T-2 toxin were hydrolysis, hydroxylation, and de-epoxidation. In addition, the results also revealed one novel metabolic pathway of T-2 toxin, hydroxylation at C-9 position, which was demonstrated by the metabolites 9-OH-T-2 and 3′,9-dihydroxy-T-2. In addition, hydroxylation at C-9 of T-2 toxin was also generated in in vitro of liver systems. Interestingly, several metabolites of hydroxylation at C-7 of T-2 toxin were also detected in in vivo male Wistar rats, but they were not found in in vivo female rats and in in vitro systems of Wistar rats.

KEYWORDS: *T-2 toxin, trichothecenes, metabolites, rat, UPLC-Q/TOF-MS*

INTRODUCTION

T-2 toxin, produced mainly by various *Fusarium* molds, attracted much attention from the whole world because it had the highest toxicity among the trichothecenes.[1,2] T-2 toxin could induce a wide range of toxic effects on both farm animals and humans because of its strong cytotoxicity,[3,4] immunotoxicity,[5,6] and reproductive toxicity.[7−9] Besides, it could cause rapid inhibition of DNA and protein synthesis.[10] The toxicity of T-2 toxin was partly attributed to its metabolites, because T-2 toxin was rapidly metabolized to various products after ingestion by organisms.[1,11] In addition, T-2 toxin posed a potential threat to humans and animals,[12,13] because it had been acknowledged as a natural contaminant in cereals such as wheat, barley, oats, maize, and animal feeds.[14] Over the years, there were numerous reports from different regions around the world describing the association of T-2 toxin with damage to agriculture and animal health.[15−17]

To have a scientific understanding on the transformation of T-2 toxin in animals and humans, the metabolism of T-2 toxin had been studied in different in vivo and in vitro experiments. In an earlier study, after incubation of T-2 toxin with hepatic microsomes of humans, rats, and chickens, it was selectively hydrolyzed at C-4, giving rise to HT-2 toxin as the only metabolite.[18,19] Subsequently, other hydrolytic metabolites of T-2 toxin such as neosolaniol (NEO), 4-deacetylneosolaniol, T-2 triol, and T-2 tetraol were identified in chicken excreta and rat hepatic homogenate.[20,21] Because the same metabolites were also obtained from HT-2 toxin used as substrate, it was concluded that T-2 toxin was hydrolyzed preferentially at the C-4 position to form HT-2 toxin, which was then metabolized to T-2 tetraol via 4-deacetylneosolaniol.[22] After oral administration of tritium-labeled T-2 toxin to a lactating cow, T-2 was rapidly metabolized in cow tissues and excreta, primarily yielding three major unknown metabolites, referred to as TC-1, TC-3, and TC-6.[23] On the basis of GC-MS and nuclear magnetic resonance (NMR) spectroscopy, they were identified 3′-hydroxy T-2, 3′-hydroxy HT-2, and 3′,7-dihydroxy HT-2, respectively, by later research.[24,25] Additionally, numerous de-epoxy metabolites such as de-epoxy-3′-hydroxy-HT-2 toxin, de-epoxy-3′-hydroxy-T-2 triol, de-epoxy-15-acetyl-T-2 tetraol, and de-epoxy T-2 tetraol were also identified in in vivo rat and cow excreta.[26,27] In addition, de-epoxy metabolites were also identified in in vitro systems of T-2 toxin incubated with rumen microorganisms.[28] In addition, phase II reaction, glucuronide conjugation of T-2 toxin and its metabolites, was also determined in in vitro and in vivo metabolism studies. Furthermore, the glucuronide conjugates accounted for approximately 70% of the total metabolite residues in in vivo swine.[29] On the analysis of these earlier metabolic studies in in vitro and in vivo different animals, such as T-2 toxin incubation with liver microsomes, primary hepatocytes, and intestinal microflora systems of animals,[30−32] the main metabolic pathways of T-2 toxin were easily conducted, followed by

Received: March 19, 2013
Revised: August 14, 2013
Accepted: August 26, 2013
Published: August 26, 2013

ACS Publications © 2013 American Chemical Society

dx.doi.org/10.1021/jf4012054 | J. Agric. Food Chem. 2013, 61, 9734−9743

hydrolysis (hydrolyzed at C-4, C-8, and C-15 positions), hydroxylation (hydroxylated at C-7, C-3′, and C-4′ positions), de-epoxidation, acetylation, and conjugation to polar moieties. Generally, T-2 toxin could be rapidly metabolized to less toxic products after ingestion by animals.[11] However, from the rat skin toxicity bioassay with 4′-hydroxy-T-2, detected in rats, mice, and chickens in vitro, this new metabolite was found to be nearly equally toxic in dermal toxicity to T-2 toxin.[1,11]

Owing to the drawback of GC-MS, some metabolites of T-2 toxin, identified mainly by GC-MS in the past, maybe could not be detected.[1,11,20−23] In the past decades, liquid chromatography−mass spectrometry (LC-MS) has evolved into the most suitable and effective tool for the analysis of metabolites, with its high speed, enhanced resolution, and greater sensitivity and specificity.[33] In this research, a sensitive UPLC-Q/TOF-MS method was applied for the structural elucidation of T-2 toxin metabolites in in vivo rats after oral administration of a single dose (3 mg/kg) of T-2 toxin. In addition, metabolites of T-2 toxin produced by liver microsomes and liver S9 fraction of male rats were also identified. The combination of the accurate mass measurements provided qualitative information from TOF date with automatic identification function of software Meabolynx^{XS}.[34] A total of 19 metabolites of T-2 toxin were identified in in vivo and in vitro systems of Wistar rats, 9 of them being novel. This work contributed to the comprehensive understanding of the metabolism of T-2 toxin in vivo and will provide an important basis for further study of its toxicological safety evaluation and marker residue finding.

MATERIALS AND METHODS

Chemicals. T-2 toxin (99%), HT-2 toxin (99%), and NEO toxin (99%) were purchased from Fermentek Ltd. (Jerusalem, Israel). β-Nicotinamide adenine dinucleotide phosphates (NADPH) was acquired from Roche Chemical Co. (Beijing, China). Ethyl acetate (analytical grade) was obtained from Sinopharm Chemical Reagent Co., Ltd. (Beijing, China). Acetonitrile (HPLC grade) was purchased from Fisher Chemical Co. (Fair Lawn, NJ, USA). Ammonia (28%) was purchased from Alfa-Aesar (Ward Hill, MA, USA). Water was purified using a Milli-Q system (Millipore, MA, USA). Cellulose sodium carboxymethyl (CMC-Na) was obtained from Guoyao Chemical Co. (Shanghai, China). All other chemicals and reagents were of the highest analytical grade available.

Animals. Male and female Wistar rats (weight = 200−250 g, 12 male and 12 female) were purchased from Vital River Laboratory Animal Technology Co. Ltd. (Beijing, China). The animals, acclimatized for 1 week in an animal room with standardized temperature (25−28 °C), humidity (50−60%), and 12 h light/dark cycle conditions before the experiment, were fed a standard diet and given water ad libitum. After a 12 h fasting and free access to water, animals were administered a single dose of T-2 toxin (3 mg/kg, adding 0.5% CMC-Na) by oral gavage. Control rats (three male and three female) were administered a similar volume of 0.5% CMC-Na solution. All care and handing of animals were performed with the approval of Institutional Authority for Laboratory Animal Care.

Preparation of Liver S9 Fraction and Hepatic Microsomes. After 12 h of fasting and free access to water, animals (three male and three female) were exsanguinated. Hepatic microsomes were prepared according to a procedure reported in previous studies.[34] The livers were rapidly removed and washed several times with ice-cold 0.1 mol/L PBS (pH 7.4) and 0.05 mol/L Tris-HCl buffer (pH 7.4) to wash away residual blood, gently blotted, and weighed. The pooled livers were minced and immediately homogenized with 3 volumes of ice-cold 0.05 mol/L Tris-HCl buffer (pH 7.4) containing 1 mmol/L EDTA and 0.25 M sucrose using a glass homogenizer. The liver S9 fraction was obtained by centrifuging the homogenate at 10000*g* for 20 min at 4 °C, and then the supernatant was collected and centrifuged at 100000*g* for 60 min at 4 °C. The microsomal pellets and the liver S9 fraction were suspended in 0.05 mol/L Tris-HCl buffer, and the protein content of the microsomes was estimated according to the method of Lowry et al. using crystalline bovine serum albumin as a standard.[35]

Preparation of Samples of in Vivo and in Vitro Systems. The urine and feces samples were collected from 0 to 24 h after oral administration. All of the samples were frozen at −20 °C before analysis. T-2 toxin and its metabolites from all samples were extracted by ethyl acetate. Twenty milliliters of ethyl acetate was added to 2 mL of urine or 2 g of feces. The mixture was vortexed for 5 min and centrifuged at 9000*g* at 4 °C for 10 min. The organic layer was transferred into a new polypropylene tube and evaporated to dryness with a gentle flow of nitrogen at 45 °C. The residue was redissolved in 0.5 mL of acetonitrile/water (15:85, v/v), and the resulting solution was centrifuged at 12000*g* at 4 °C for 15 min. Finally, the supernatant was filtered through a 0.22 μm microbore cellulose membrane into an autosampler vial and analyzed by UPLC-Q/TOF-MS for identification of metabolites.

The incubation mixture (total volume = 500 μL) consisting of 2 mg protein/mL of liver S9 fraction or liver microsomes (the volume was 447.5 μL) and 2 mmol/L NADPH-generating system (the volume was 50 μL) was preincubated for 5 min at 37 °C. The reaction was initiated thereafter by the addition of 2.5 μL of T-2 toxin (10 mmol/L). Incubation mixtures without T-2 toxin and a NADPH-generating system served as controls. After 2 h of incubation at 37 °C in a metabolic shaker, the reaction was terminated by adding 500 μL of ice-cold ethyl acetate. After volution and centrifugation at 12000 rpm at 4 °C for 15 min, the supernatant was filtered through a 0.22 μm microbore cellulose membrane into an autosampler vial and analyzed by UPLC-Q/TOF-MS for identification of metabolites.

Instrumental Conditions. Identification of T-2 toxin metabolites was conducted by using an ACQUITY UPLC system (Waters Co., Milford, MA, USA) coupled with a hybrid Q-TOF-MS SYNAPT HDMS (Waters, Manchester, UK). Chromatographic separation of metabolites of T-2 toxin was performed on the ACQUITY ultraperformance liquid chromatography system with ambient temperature, using an Acquity BEH RP18 column (50 mm × 2.1 mm i.d., 1.7 μm particle size) (Waters, Milford, MA, USA). The mobile phase consisting of water with 0.005 mmol/L ammonia (solvent A) and acetonitrile (solvent B) was pumped at a flow rate of 0.3 mL/min. The gradient elution program was as follows: 0−1.0 min, 2−5% B; 1.0−7.0 min, 5−60% B; 7.0−10.0 min, 60−100% B; 10.0−11.0 min, 100% B; 11.0−12.5 min, 100−2% B; 12.5−13.0 min, equilibration of the column. The volume of sample injected was 10 μL.

The UPLC system was coupled to a hybrid electrospray ionization quadrupole time-of-flight mass spectrometer (SYNAPT High-Definition Mass Spectrometry system; Waters, Milford, MA, USA). Typical source conditions for maximum intensity of precursor ions were as follows: capillary voltage, 3.0 kV; source temperature, 120 °C; desolvation temperature, 300 °C; cone gas (N_2) flow rate, 20 L/h; desolvation gas (N_2) flow rate, 700 L/h. The argon pressure in the collision cell was 3.5×10^{-3} mbar. For parent toxin and metabolites, ESI source was operated in the positive ionization mode. Data were acquired from 100 to 700 Da and centroided during acquisition using an internal reference comprising a 1 ng/μL solution of leucine enkephalin infused at 50 μL/min, generating a reference ion in ESI positive ionization mode at m/z 556.2771. Low-energy data were acquired at the collision energy of 5 eV and high-energy data using the ramped collision energy of 10−30 eV.

Data Processing. Data processing was carried out using Metabolynx^{XS} software (version 4.1), which can automatically identify metabolites by comparing the sample with the control. The parameters were adjusted as shown in Table 1.

RESULTS AND DISCUSSION

Mass Spectrometric Analysis of T-2 Toxin. Initially, it was critical to figure out the fragmentation pathways of T-2 toxin, because its metabolites had the corresponding

dx.doi.org/10.1021/jf4012054 | J. Agric. Food Chem. 2013, 61, 9734−9743

Table 1. Presetting Parameters of Metabolynx^{XS} Software

parameter	setting
MS trace condition	retention time range
expected metabolite chromatograms	mass value of parent compound
unexpected metabolite chromatograms	full acquisition range (100−700 Da)
smooth mode	Savitzky−Golay (1 × 1)
absolute area	10
spectrum condition	combined mode
	minimum peak separation (0.05 Da)
	intensity threshold (10%)
false-positive condition	isotope entries (mass window 5.0 Da)
	mass window (0.05 Da)
	retention time (0.1 min)
mass defect fliter (MDF)	±50 mDa

fragmentation pathways to T-2 toxin in MS/MS spectra ($[M + NH_4]^+$). T-2 toxin was eluted at a retention time of 6.29 min, and Table 2 lists elemental compositions, observed and calculated masses, and mass errors of T-2 toxin with NH_4^+ and its fragment ions. The differences between the measured and calculated masses with relatively good accuracy ranged from −2.3 to 3.0 mDa (−12.4 to 6.2 ppm), and accurate mass ensured high confidence for the structures of product ions. The MS/MS spectrum of T-2 toxin is shown in Figure 1. T-2 toxin with NH_4^+ at m/z 484 lost an $NH_3{\cdot}H_2O$ to form m/z 449 and further form m/z 409 by losing C_2H_2O; or T-2 toxin lost $C_5H_{12}O_2$ and NH_3 to form m/z 365 and then generated the main fragment ion at m/z 305 by losing $C_2H_4O_2$. The fragment at m/z 305 generated m/z 245 or 275 with the absence CH_2O or $C_2H_4O_2$, respectively, and at last form another main fragment ion at m/z 215. The fragment at m/z 215 lost successively H_2O or CH_2O to form m/z 197 or 185, respectively. Subsequently, the fragment at m/z 169 was generated by the loss of O radical from the fragment at m/z 185. According to the results above, the fragmentation pathways of T-2 toxin are as proposed in Figure 2.

Table 2. Elemental Composition, Measured and Exact Masses, Double-Bond Equivalents (DBE), and Corresponding Mass Errors of T-2 Toxin with NH_4^+ and Its Fragment Ions

elemental composition	measured mass (Da)	accurate mass (Da)	DBE	mass error (mDa)	corresponding mass error (ppm)
$C_{24}H_{38}NO_9^+$	484.2577	484.2547	6.5	3.0	6.2
$C_{24}H_{33}O_8^+$	449.2184	449.2175	8.5	0.9	2.0
$C_{22}H_{31}O_7^+$	407.2052	407.2070	7.5	−1.8	−4.4
$C_{19}H_{25}O_7^+$	365.1584	365.1600	7.5	−1.6	−4.4
$C_{17}H_{21}O_5^+$	305.1371	305.1389	7.5	−1.8	−5.9
$C_{16}H_{19}O_4^+$	275.1274	275.1283	7.5	−0.9	−3.4
$C_{15}H_{17}O_3^+$	245.1162	245.1178	7.5	−1.6	−6.5
$C_{14}H_{15}O_2^+$	215.1049	215.1072	7.5	−2.3	−10.7
$C_{14}H_{13}O^+$	197.0948	197.0966	8.5	−1.8	−9.1
$C_{13}H_{13}O^+$	185.0943	185.0966	7.5	−2.3	−12.4
$C_{13}H_{13}^+$	169.1001	169.1017	7.5	−1.6	−9.5

Identification of T-2 Toxin Metabolites. Metabolynx^{XS} software automatically compared MS^E LC-MS data of the sample and control by presetting the parameters. The proposed metabolites were listed by the software and were analyzed using the MS/MS mode for the further confirmation.[34] As shown in the Table 2, there were totally 19 metabolites of T-2 toxin discovered in vivo and in vitro. Metabolites T1, T2, T4, T5, T6, T7, T9, T10, T15, and T16 had been reported in previous studies, which were consistent with the earlier metabolic reports on T-2 toxin,[1,11,14] whereas the other metabolites were first discovered in this research, such as 15-deacetyl-T-2, 3′-OH-15-deacetyl-T-2, 3′,7-dihydroxy-T-2, isomer of 3′,7-dihydroxy-T-2, 7-OH-HT-2, isomer of 7-OH-HT-2, de-epoxy-3′,7-dihydroxy-HT-2, 9-OH-T-2, and 3′,9-dihydroxy-T-2 (Table 3). The extracted mass chromatograms (EIC) and the mass spectra of all the metabolites of T-2 toxin detected are shown in Figures 3 and 4, respectively.

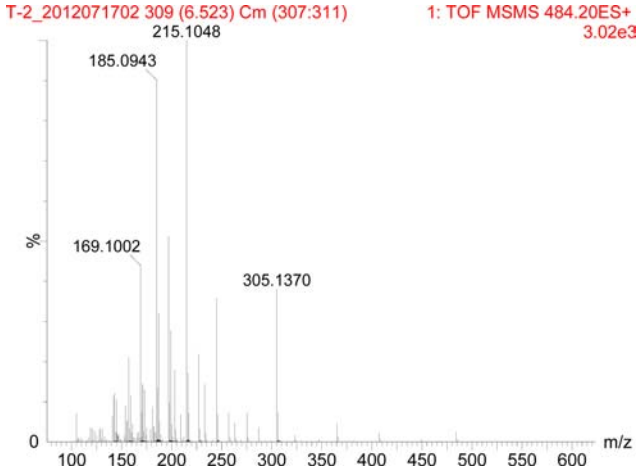

Figure 1. Accurate MS/MS spectra of T-2 toxin.

Metabolites T1 and T3. Metabolites T1 and T3 were eluted at 5.43 and 4.70 min, respectively, and showed the same $[M + NH_4]^+$ ions at m/z 442.2425 with the elemental composition of $C_{22}H_{36}NO_8$, which was 42 Da less than T-2 toxin with NH_4^+ at m/z 484, suggesting that they were metabolites of T-2 toxin without acetyl groups. The difference between T1 and T3 lay in the position of acetyl group reduction, because their retention times were different. Fragment ions from the MS/MS spectrum of T1 were m/z 442, 323, 263, and 233, which were 42 Da less than the m/z 484, 365, 305, and 275 of T-2 toxin, respectively, further suggesting that T1 was a metabolite of T-2 toxin without an acetyl group. Besides, metabolite T1 was the same as HT-2 toxin in both retention time and fragment ions. Therefore, metabolite T1 was identified as HT-2 toxin.

As to the metabolite T3, the main fragment ions at m/z 305 and 245 were identical to those of T-2 toxin, suggesting there was the same structure between the metabolite T3 and T-2 toxin. In addition, because there were two acetyl groups at C-4 and C-15 in the T-2 toxin, one metabolite without acetyl group at C-4 was identified as HT-2, and another should be at C-15. Therefore, metabolite T3 was identified as 15-deacetyl-T-2.

Metabolite T2. Metabolite T2 was eluted at 3.34 min and showed an $[M + NH_4]^+$ ion at m/z 400.1957 with the elemental composition of $C_{19}H_{30}NO_8$, which was 84 Da less than T-2 toxin with NH_4^+ at m/z 484, suggesting that it was a metabolite of T-2 toxin without the isovaleryl at the C-8 position. Fragment ions from the MS/MS spectrum of T2 were m/z 365, 305, 275, 257, 245, 215, and 185, which were identical to T-2 toxin. In addition, T2 was the same as NEO toxin in both retention time and fragment ions. Consequently, metabolite T2 was identified as NEO toxin.

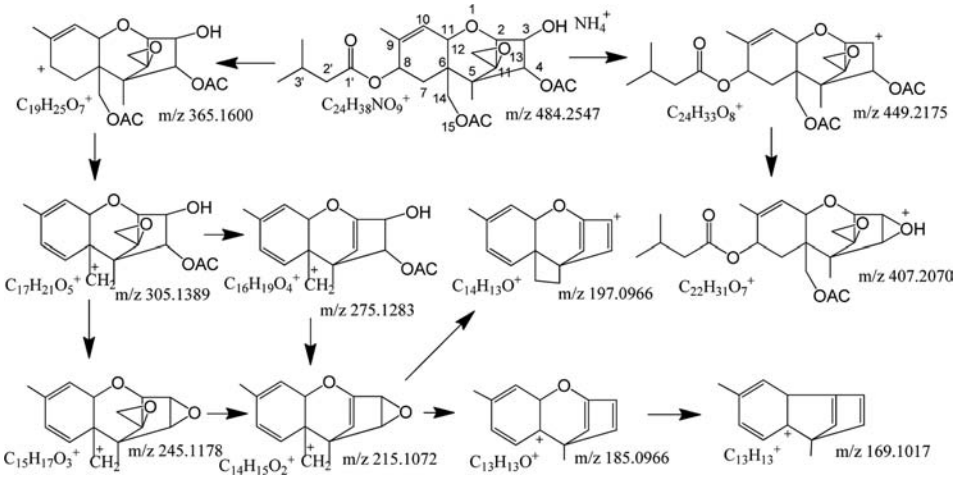

Figure 2. Proposed fragmentation pathways of T-2 toxin.

Table 3. Summary of Metabolites of T-2 Toxin Identified in in Vivo and in Vitro Systems

metabolite	$[M + NH_4]^+$ (m/z)	mass error (mDa)	retention time (min)	molecular formula	ppoposed structure	major fragments[a]
T0	484.2547	2.1	6.52	$C_{24}H_{38}NO_9^+$	T-2 toxin	484, 449, 407, 365, 305, 275, 245, 205, 197, **185**, 169
T1	442.2441	1.6	5.43	$C_{22}H_{36}NO_8^+$	HT-2 toxin	442, 425, 323, 305, **263**, 245, 215, 197, 169
T2	400.1971	−1.4	3.34	$C_{19}H_{30}NO_8^+$	NEO toxin	400, 305, 257, 245, **215**, 185, 169
T3	442.2441	1.4	4.73	$C_{22}H_{36}NO_8^+$	15-deacetyl-T-2	442, 425, 305, 263, 245, **227**, 199, 187
T4	358.1866	−1.2	1.95	$C_{17}H_{28}NO_7^+$	4-deacetylneosolaniol	358, 323, **263**, 245, 215, 197, 169, 157
T5	358.1866	−2.8	2.93	$C_{17}H_{28}NO_7^+$	15-deacetylneosolaniol	358, 323, 263, 245, 233, **215**, 185, 157
T6	500.2496	0.9	4.63	$C_{24}H_{38}NO_{10}^+$	3′-OH-T-2	500, 245, 215, 197, **185**, 169
T7	458.2390	−1.9	3.76	$C_{22}H_{36}NO_9^+$	3′-OH-HT-2	458, 323, 263, 245, 227, 215, **197**, 185, 157
T8	458.2390	−2.9	3.49	$C_{22}H_{36}NO_9^+$	3′-OH-15-deacetyl-T-2	458, 323, **305**, 287, 245, 227, 199
T9	474.2339	1.3	2.92	$C_{22}H_{36}NO_{10}^+$	3′,7-di-OH-HT-2	474, 397, 379, 279, 261, **249**, 231, 185
T10	474.2339	1.9	3.16	$C_{22}H_{36}NO_{10}^+$	isomer of 3′,7-di-OH-HT-2	474, 397, 379, 279, 261, **249**, 231, 185
T11	516.2445	−1.3	3.89	$C_{24}H_{38}NO_{11}^+$	3′,7-di-OH-T-2	516, 481, 421, 381, 321, **291**, 182
T12	516.2445	−1.4	4.08	$C_{22}H_{36}NO_{11}^+$	isomer of 3′,7-di-OH-T-2	516, 481, 421, 381, 321, **291**, 182
T13	458.2390	−2.2	4.47	$C_{22}H_{36}NO_9^+$	7-OH-HT-2	458, 441, 423, 339, 321, 279, 261, **249**, 231, 213, 189
T14	458.2390	−1.8	4.77	$C_{22}H_{36}NO_9^+$	isomer of 7-OH-HT-2	458, 441, 423, 339, 321, 279, 261, **249**, 231, 213, 189
T15	442.2441	−2.1	4.09	$C_{22}H_{36}NO_8^+$	de-epoxy-3′-OH-HT-2	442, 407, 289, 247, **229**, 211, 201, 193, 183
T16	426.2493	−2.3	5.74	$C_{22}H_{36}NO_7^+$	de-epoxy-HT-2	426, 409, 307, 289, 247, 229, **211**, 201, 193, 183
T17	458.2390	−1.5	3.31	$C_{22}H_{36}NO_9^+$	de-epoxy-3′,7-di-OH-HT-2	458, **423**, 405, 363, 345, 327, 305, 263, 245, 227, 203
T18	502.2652	1.1	5.00	$C_{24}H_{40}NO_{10}^+$	9-OH-T-2	502, 425, **383**, 305, 263, 245, 227, 197
T19	518.2584	−1.8	3.60	$C_{24}H_{40}NO_{11}^+$	3′-OH-9-OH-T-2	518, 483, 443, 425, 399, 381, 323, 305, 281, **263**, 245,

[a]The base peak in the MS/MS spectra is shown in boldface type.

Metabolites T4 and T5. Metabolites T4 and T5 were eluted at 1.95 and 2.93 min, respectively, and they showed the same $[M + NH_4]^+$ ions at m/z 358.1854 with the elemental composition of $C_{17}H_{28}NO_7$, which was 42 Da less than NEO toxin with NH_4^+ at m/z 400, suggesting that they were metabolites of NEO toxin without one acetyl group. From the MS/MS spectrum between metabolite T4 and HT-2 toxin, the fragments of m/z 305, 263, 245, 233, 227, 215, 197, and 185 were the same fragments with similar abundances, implying that metabolite T4 was the acetyl group reduced at C-4 metabolite of NEO toxin.

Metabolite T5 with NH_4^+ at m/z 358 lost an $NH_3{\cdot}H_2O$ to form m/z 323. The fragments at m/z 305 or 293 were formed by successively losing H_2O or CH_2O from m/z 323. Subsequently, the fragment at m/z 263 forms m/z 245, 233, 227, 215, 197, and 187, successively, as happened with the same cataclastic behavior of m/z 263 in HT-2 toxin. Although there were the same ion fragments between metabolite T5 and HT-2 toxin, the abundances of the ion fragments were very different. Therefore, metabolites T4 and T5 were identified as 4-deacetylneosolaniol and 15-deacetylneosolaniol, respectively.

Metabolite T6. Metabolite T6 showed an $[M + NH_4]^+$ ion at m/z 500.2487 with the elemental composition of $C_{24}H_{38}NO_{10}$, which was 16 Da higher than T-2 toxin, indicating that it was the hydroxylation metabolite of T-2 toxin. Fragment ions from the MS/MS spectrum of T6 were m/z 365, 305, 275,

dx.doi.org/10.1021/jf4012054 | J. Agric. Food Chem. 2013, 61, 9734−9743

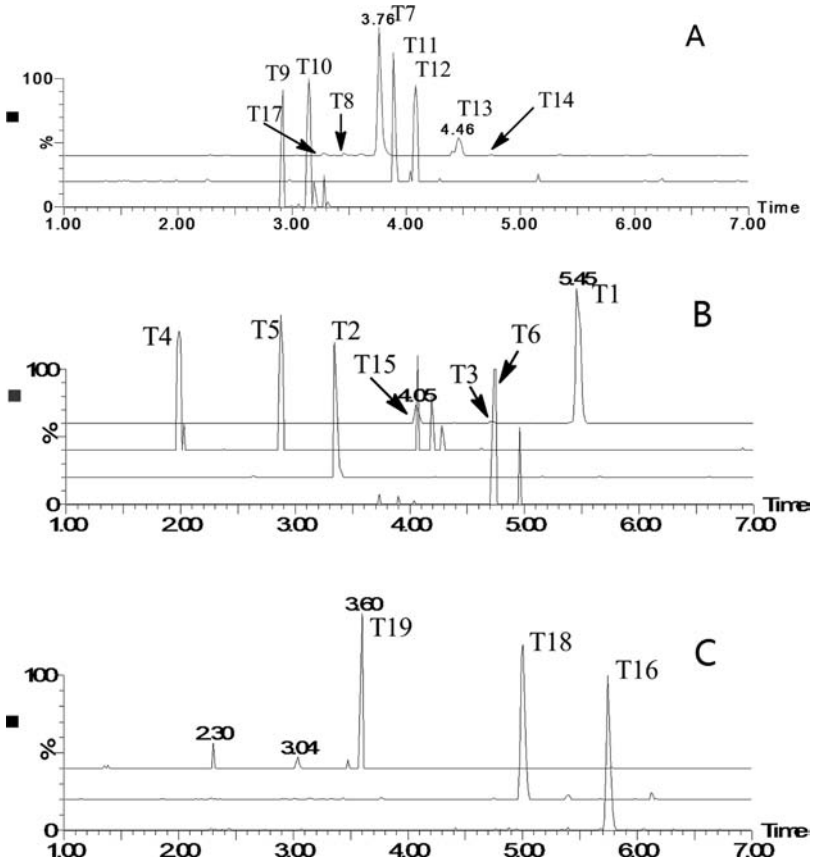

Figure 3. Extracted mass chromatography of the metabolites of T-2 toxin detected in in vivo and in vitro systems.

257, 245, 215, and 185, which was identical to T-2 toxin. T6 with NH_4^+ at *m/z* 500 generated *m/z* 483 and 365 by losing successively NH_3 and $C_5H_{12}O_3$, suggesting that the isovaleryl at the C-8 position had been hydrolyzed. Therefore, T6 was identified as 3′-OH-T-2.

Metabolites T7 and T8. Metabolites T7 and T8 were eluted at 3.76 and 3.49 min, respectively. Both metabolites showed the same $[M + NH_4]^+$ ions at *m/z* 458.2371 with the same elemental composition of $C_{22}H_{36}NO_9$, which was 16 Da higher than HT-2 toxin, implying that they were hydroxylated metabolites of HT-2 toxin or 15-deacetyl-T-2. Fragments of metabolite T7 were *m/z* 323, 263, 245, 233, 215, 197, 185, and 169, which were identical to those of HT-2 toxin. In addition, metabolite T7 with NH_4^+ at *m/z* 458 lost NH_3 to form *m/z* 441 and then lost $C_5H_{10}O_3$ to form *m/z* 323, suggesting that the isovaleryl at the C-8 position had been hydrolyzed. Thus, metabolite T7 was identified as 3′-OH-HT-2.

Fragments of metabolite T8 were *m/z* 305, 263, 245, 227, 199, and 187, which were identical to those of 15-deacetyl-T-2. In addition, metabolite T8 with NH_4^+ at *m/z* 458 lost an $NH_3 \cdot H_2O$ to form *m/z* 423 and then lost $C_5H_{10}O_3$ to form *m/z* 305, suggesting that the isovaleryl at the C-8 position had been hydrolyzed. Consequently, metabolite T8 was identified as 3′-OH-15-deacetyl-T-2.

Metabolites T9 and T10. Metabolites T9 and T10 were eluted at 2.92 and 3.16 min, respectively. Both metabolites showed the same $[M + NH_4]^+$ ions at *m/z* 474.2326 with the same elemental composition of $C_{22}H_{36}NO_{10}$, which was 16 Da higher than 3′-OH-HT-2, implying that they were hydroxylation metabolites of 3′-OH-HT-2. Fragments of metabolite T9 were *m/z* 474, 249, 279, and 379, which were 16 Da higher than the fragments at *m/z* 458, 265, 295, and 395 of 3′-OH-HT-2, respectively, further suggesting that metabolite T9 was a hydroxylated metabolite of 3′-OH-HT-2. The fragment *m/z* 305 was generated by losing $C_5H_8O_2$ from *m/z* 421, suggesting that the isovaleryl was hydrolyzed. According to the obtained results, T9 was identified as 3′,7-dihydroxy-HT-2.

The metabolite T10 had the same fragment ions as metabolite T9, whereas their retention times were different, indicating they were the isomers of 3′,7-dihydroxy-HT-2.

Metabolites T11 and T12. Metabolites T11 and T12 were eluted at 3.89 and 4.08 min, respectively, and showed the same $[M + NH_4]^+$ ions at *m/z* 516.2432 with the same elemental composition of $C_{24}H_{38}NO_{11}$, which was 42 Da higher than 3′,7-dihydroxy-HT-2, implying that they were acetylated metabolites of 3′,7-dihydroxy-HT-2. Fragments of metabolite T11 were *m/z* 516, 481, 463, 421, 321, and 279, which were 42 Da higher than the fragments at *m/z* 474, 439, 421, 379, 279, and 249 of 3′,7-dihydroxy-HT-2, respectively, further suggesting that T11 was the acetylated metabolite of 3′,7-dihydroxy-HT-2. Therefore, T11 was identified as 3′,7-dihydroxy-T-2. Metabolite T12 had the same fragment ions as T11, but their retention times were different, indicating they were the isomers of 3′,7-dihydroxy-T-2.

Metabolites T13 and T14. Metabolites T13 and T14 were eluted at 4.47 and 4.77 min, respectively. Both metabolites showed the same $[M + NH_4]^+$ ions at *m/z* 458.2378 with the same elemental composition of $C_{22}H_{36}NO_9$, which was 16 Da less than 3′,7-dihydroxy-HT-2, implying that they were dehydroxylation metabolites of 3′,7-dihydroxy-HT-2. The fragments of T13 were *m/z* 458, 439, and 379, which were 16 Da less than *m/z* 474, 439, and 379 of 3′,7-dihydroxy-HT-2,

dx.doi.org/10.1021/jf4012054 | J. Agric. Food Chem. 2013, 61, 9734−9743

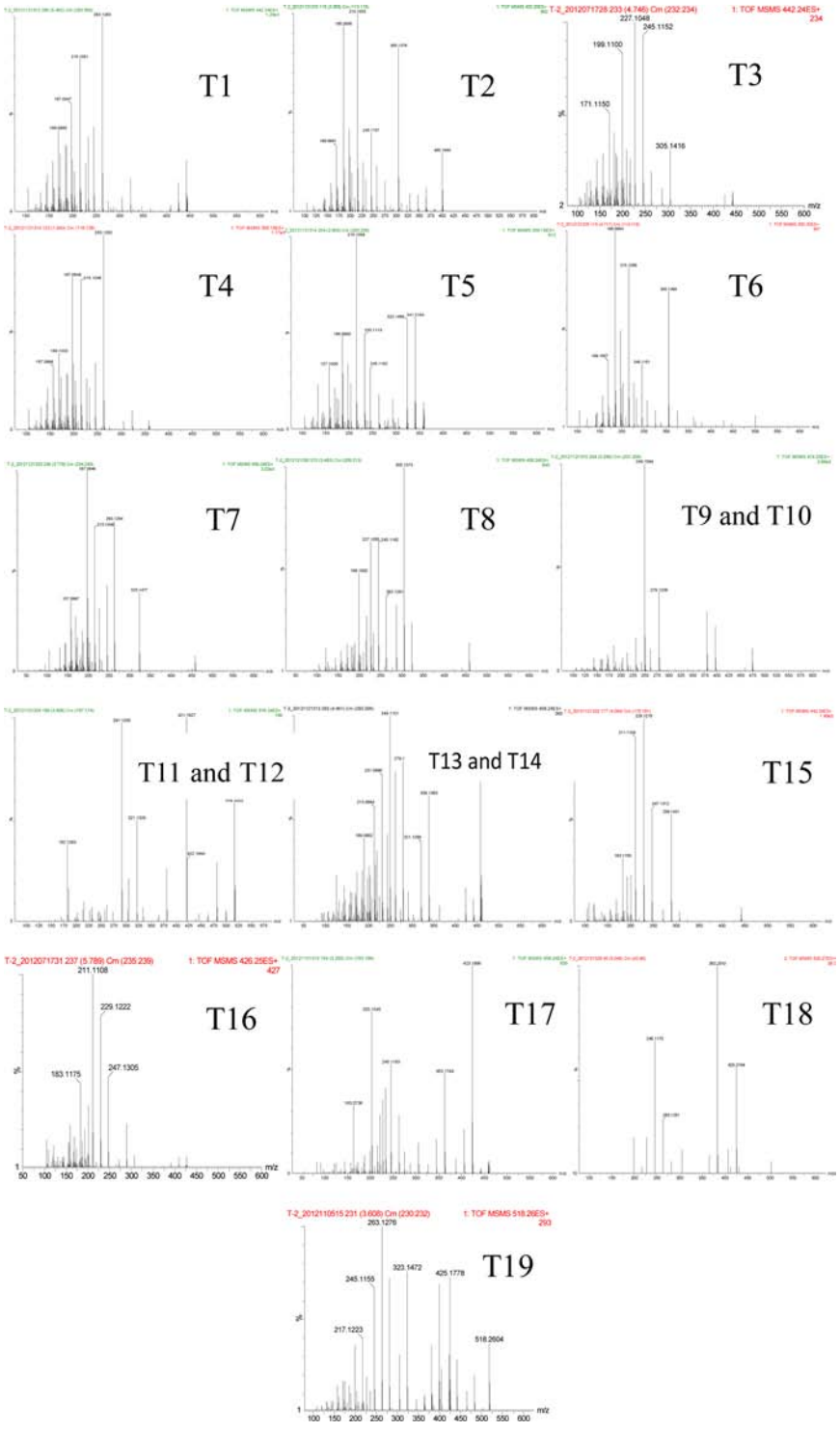

Figure 4. MS/MS spectra of the metabolites of T-2 toxin detected in in vivo and in vitro systems of rats.

respectively. Additionally, the fragment at m/z 423 generated m/z 321 by losing $C_5H_{10}O_2$, implying that the isovaleryl was not changed yet, which further suggested that T13 should be 7-OH-HT-2. Metabolite T14 had the same fragment ions as T13, but was eluted at a different retention time, indicating they were isomers of each other.

Metabolite T15. Metabolite T15 was eluted at the retention time of 4.09 min and showed an $[M + NH_4]^+$ ion at m/z 442.2420 with the elemental composition of $C_{22}H_{36}NO_8$, which was 16 Da less than metabolite T7 of 3′-OH-HT-2, implying it was a de-epoxy metabolite of 3′-OH-HT-2. The fragments of T15 were m/z 442, 247, 229, and 211, which were 16 Da less than m/z 458, 263, 245, and 227 of 3′-OH-HT-2, respectively, further suggesting that T15 was the de-epoxy metabolite of 3′-OH-HT-2. In addition, the fragment at m/z 307 was generated by losing $C_5H_8O_2$ from m/z 407, suggesting that the isovaleryl was not changed yet. According to the results obtained, metabolite T15 was identified as de-epoxy 3′-OH-HT-2.

dx.doi.org/10.1021/jf4012054 | J. Agric. Food Chem. 2013, 61, 9734−9743

Metabolite T16. Metabolite T16 was eluted at 5.74 min and showed an $[M + NH_4]^+$ ion at m/z 426.2470 with the elemental composition of $C_{22}H_{36}NO_7$, which was 16 Da less than metabolite T15 of de-epoxy 3′-OH-HT-2, implying that it was the dehydroxylation metabolite of de-epoxy 3′-OH-HT-2. The fragmens of T16 were m/z 307, 289, 247, 229, 201, and 183, which were identical to de-epoxy 3′-OH-HT-2. Furthermore, the fragment at m/z 409 forms m/z 307 by losing $C_5H_{10}O_2$, suggesting that the isovaleryl remained unchanged. Consequently, metabolite T16 was identified as de-epoxy HT-2.

Metabolite T17. Metabolite T17 was eluted at 3.31 min and showed an $[M + NH_4]^+$ ion at m/z 458.2375 with the elemental composition of $C_{22}H_{36}NO_9$, which was 16 Da less than metabolites T9 and T10 of 3′,7-dihydroxy-HT-2, implying that it was a de-epoxy metabolite of 3′,7-dihydroxy-HT-2. The fragments of metabolite T17 were m/z 458, 423, 405, 363, 263, 245, 233, and 227, which were 16 Da less than the fragments at m/z 474, 439, 421, 379, 279, 261, 249, and 243 of 3′,7-dihydroxy-HT-2, respectively, further suggesting that it was the de-epoxy metabolite of 3′,7-dihydroxy-HT-2.

Metabolite T18. Metabolite T18 was eluted at 5.00 min and showed an $[M + NH_4]^+$ ion at m/z 502.2641 with the elemental composition of $C_{24}H_{40}NO_{10}$, which was 18 Da higher than T-2 toxin, implying that the hydroxylation maybe occurred at the C-9 or C-10 position of T-2 toxin. Fragment ions from the MS/MS spectrum of T18 were m/z 502, 467, 425, 383, 323, and 263, which were 18 Da higher than m/z 484, 449, 407, 365, 303, and 245 of T-2 toxin, respectively, further suggesting that the hydroxylation occurred at the C-9 or C-10 position of T-2 toxin. The fragment at m/z 425 formed m/z 323 by losing $C_5H_{10}O_2$, implying the isovaleryl was not changed yet. Additionally, there would be isomers for metabolite T18, if the hydroxylation occurred at the C-10 position of T-2 toxin. However, only one metabolite was detected in this study, suggesting that the hydroxylation occurred at C-9. Therefore, metabolite T18 was identified as 9-OH-T-2.

Metabolite T19. Metabolite T19 was eluted at 3.60 min and showed an $[M + NH_4]^+$ ion at m/z 518.2566 with the elemental composition of $C_{24}H_{40}NO_{11}$, which was 16 Da higher than 9-OH-T-2, indicating that it may be the hydroxylation metabolite of 9-OH-T-2. The fragments of T19 at m/z 467, 425, 383, 323, 305, 263, 245, 217, and 199 were identical to the those of metabolite T18. Additionally, the fragment at m/z 483 formed m/z 365 by losing $C_5H_{12}O_3$, suggesting that the isovaleryl was hydrolyzed. Consequently, metabolite T19 was identified as 3′,9-dihydroxy-OH-T-2.

Metabolic Pathways of T-2 Toxin. T-2 toxin was easily hydrolyzed in in vivo and in vitro systems, because there were three ester bonds, including at the C-4, C-15, and C-8 positions of T-2 toxin. Various metabolites were generated by hydrolysis at different positions of ester bonds. However, the capability of hydrolysis was different at different positions of the three ester bonds, so that there was a tremendous difference in the amounts of hydrolyzed metabolites.[1,11] In the present study, the results in vivo of rats showed that the amount of HT-2 toxin was most, followed by NEO toxin and 4-deacetylneosolaniol, and the least was 15-deacetyl-T-2 and 15-deacetylneosolaniol, suggesting that the ester bond at the C-4 position was more easily hydrolyzed than that at C-15 and C-8 of T-2 toxin. Besides, T-2 toxin incubated with liver microsomes and liver S9 fraction also confirmed the above viewpoint, because the amount of HT-2 toxin far outweighed NEO and 4-deacetylneosolaniol. However, T-2 triol and T-2 tetraol, reported by previous research,[20,21] were not detected in this study, which may be too low in quantity to be detected. Among the hydrolyzed metabolites detected in in vivo rats, 15-deacetyl-T-2 and 3′-OH-15-deacetyl-T-2 were first detected, but they were not detected in in vitro systems.

Hydroxylation is another important pathway for T-2 toxin. After chemical intrusion into the body, it is prone to be oxidized by the mixed-function oxidase. Hydroxylation at C-3′ and C-4′ of isovaleryl of T-2 toxin had been reported in previous studies.[24,32] The metabolites of hydroxylation at C-3′ had been detected in in vivo and in vitro systems, whereas hydroxylation at C-4′ was detected only in vitro. Furthermore, the toxicity of 4′-OH-T-2 was found to be greater than that of 3′-hydroxy-T-2 and nearly equal in dermal toxicity to T-2 toxin, indicating that hydroxylation of T-2 toxin at the C-4′ position was not a detoxification reaction.[1,11] In our study, many metabolites of hydroxylation at C-3′ were also detected, including 3′-OH-T-2, 3′-OH-HT-2, 3′-OH-15-deacetyl-T-2, and so on, whereas 3′-OH-T-2 triol, reported by a previous study,[11] was not found in this research. Additionally, there was also one metabolite of hydroxylation at C-3′, 3′-OH-T-2, in small amount, detected in in vitro systems. The above results showed that the capacity of hydroxylation at the C-3′ position in vivo was more powerful than in in vitro systems. Besides, metabolites of hydroxylation at C-4′ were not found in in vivo and in vitro studies. It is noteworthy that one new metabolite of hydroxylation at C-3′, 3′-OH-15-deacetyl-T-2, was found in in vivo study, with the nearly equal amount of 3′-OH-T-2.

One novel metabolic pathway of T-2 toxin, hydroxylation at C-9, was found first in in vivo and in vitro systems. There were two new metabolites, 9-OH-T-2 and 3′,7-dihydroxy-T-2, detected and identified in in vivo Wistsr rats. Besides, the amount of 9-OH-T-2 was almost equal to that of NEO toxin. However, there was only one metabolite of hydroxylation at C-9, 9-OH-T-2, detected in in vitro systems. In addition, the amount of 9-OH-T-2 in the systems of live S9 fraction was more abundant than in live microsomes. The experimental results in vitro of T-2 toxin showed that hydroxylation at C-9 of T-2 toxin could be metabolized by the liver systems. To better assess the harm of T-2 toxin for animals and people, the toxicological properties of new metabolites of hydroxylation at C-9 of T-2 toxin are urgently needed to be clarified in future studies.

Hydroxylation at C-7, another novel metabolic pathway of T-2 toxin, was first detected in in vivo Wister rats, whereas it was not found in in vitro systems. Various metabolites of hydroxylation at C-7 of T-2 toxin were detected and identified in in vivo male rats, including 7-OH-HT-2, 3′,7-dihydroxy-T-2, 3′,7-dihydroxy-HT-2, and their isomers as well as de-epoxy-3′,7-dihydroxy-HT-2. Numerous metabolites of hydroxylation at C-7 of T-2 toxin demonstrated that hydroxylation at C-7 was a significant metabolic pathway for T-2 toxin. Furthermore, the amount of 3′,7-dihydroxy-HT-2 was more than HT-2 toxin in vivo male rats. Interestingly, this novel metabolic pathway of T-2 toxin, hydroxylation at C-7, was not found in in vivo female rats yet, because there was no metabolite of hydroxylation at C-7 detected in female rats. Is the novel metabolic pathway of T-2 toxin, hydroxylation at C-7, metabolized by the liver systems or by extrahepatic systems? Why was there a significant difference between male and female rats? The liver metabolic enzymes, which are different in males and females, should be partly responsible for it. Further experiments are urgently needed to

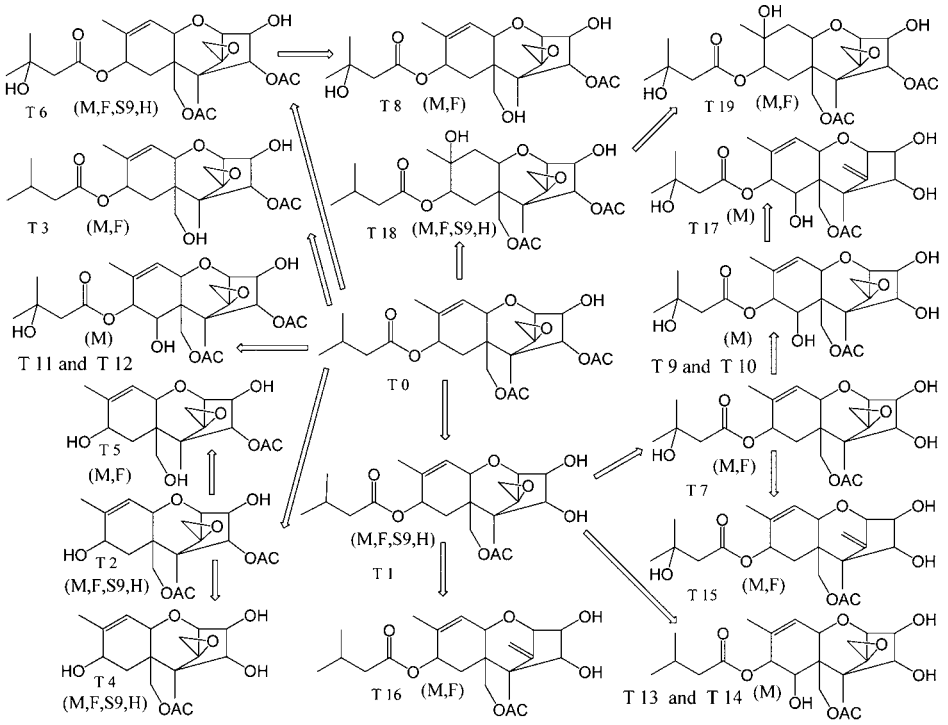

Figure 5. Metabolic pathways of T-2 toxin in in vivo and in vitro systems of Wistar rats.

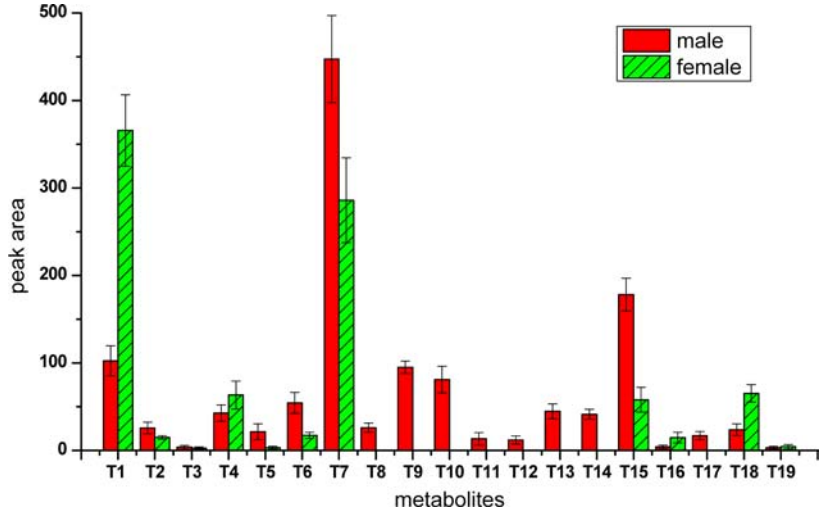

Figure 6. Relative amounts of various metabolites of T-2 toxin in in vivo of male and female rats.

answer these questions. Early studies, the metabolism of T-2 toxin in cattle, showed that hydroxylation at C-7 of T-2 toxin could happen, because there was one metabolite, 3′,7-dihydroxy-HT-2, detected and identified by GC-MS and NMR spectroscopy.[23] Besides, the authors believe that hydroxylation at C-7 of T-2 toxin may be metabolized by rumen microorganisms of ruminants, because there were various microorganisms in the rumen of ruminants. The results of this study showed that hydroxylation at C-7 of T-2 toxin could also occur in nonruminants. Furthermore, the amount of metabolites of hydroxylation at C-7 of T-2 toxin was remarkable. The toxicological properties of new metabolites of T-2 toxin were urgently needed to further research.

The de-epoxidation of T-2 toxin, an effective detoxification for T-2 toxin, had been clarified in a previous study.[26] In in vitro systems, T-2 toxin incubated with gut microbes demonstrated that the de-epoxidation of T-2 toxin was metabolized by anaerobic microorganisms in the intestine.[11] Of course, there were lots of metabolites of de-epoxidation of T-2 toxin detected in in vivo male and female rats, including de-epoxy-HT-2, de-epoxy-3′-OH-HT-2, de-epoxy-3′-OH-15-de-acetyl-T-2, and de-epoxy-3′,7-dihydroxy-HT-2, suggesting that de-epoxidation of T-2 toxin was an important metabolic pathway in vivo. However, none of the de-epoxidase metabolites was detected in in vitro liver systems, which once

dx.doi.org/10.1021/jf4012054 | J. Agric. Food Chem. 2013, 61, 9734−9743

again proved that the de-epoxidation of T-2 toxin was not metabolized by the liver systems.

On the basis of the above, the main metabolic pathways of T-2 toxin in in vivo and in vitro Wistar rats were concluded, which was hydrolysis (hydrolyzed at C-4, C-8, and C-15 positions), hydroxylation (hydroxylated at C-7, C-9, and C-3′ positions), and de-epoxidation. Additionally, the metabolic pathway of T-2 toxin is shown in Figure 5

Comparison Metabolism of T-2 Toxin in in Vivo and in Vitro Systems. After identification of metabolites of T-2 toxin, it was necessary to quantify the detected metabolites. Only in this way could we determine what were the major metabolites and secondary metabolites. To further understand the toxicological properties and other aspects, chemical synthesis of those major metabolites was necessary. Considering the matrix effects and the limit detection of the instrument in this study, we could approximately quantify the detected metabolites. Nevertheless, quantification of the metabolite of T-2 toxin was still meaningful. From various samples of in vivo study, the urine samples were found to have higher levels of metabolites and less impurity. Therefore, the 0−24 h urine samples after rats administered T-2 toxin were collected, because there were little metabolites detected after 24 h.[1,14] To reduce the impact of the individual differences, the urine of the mixed multirats was adopted. It turned out that hydrolysis, hydroxylation, and de-epoxidation were the major metabolic pathways of T-2 toxin in in vivo studies, whereas the conjugation metabolite of T-2 toxin was not detected, which is shown in Figure 5. The metabolic studies of T-2 toxin in in vivo male rats showed that the main metabolites were 3′-OH-HT-2, de-epoxy-3′-OH-HT-2, 3′,7-dihydroxy-HT-2, HT-2, 3′-OH-T-2, 4-deacetylneosolaniol, and 7-OH-HT-2, sequentially. It is worthy of noting that there was a significant difference between male and female rats in the metabolites of T-2 toxin, because hydroxylation at C-7 of T-2 toxin could not occur in female rats. HT-2, 3′-OH-HT-2, de-epoxy-3′-OH-HT-2, 3′-OH-T-2, 9-OH-T-2, and 4-deacetylneosolaniol were the main metabolites for female rats. The detailed amounts of various metabolites of T-2 toxin in male and female rats is shown in Figure 6.

After 2 h of incubation, the samples of in vitro systems, T-2 toxin incubated with liver microsomes and liver S9 fraction, were used for quantitative study of metabolites after simple pretreatment. It turned out that hydrolysis was the main metabolic pathway of T-2 toxin in in vitro systems, followed by hydroxylation. HT-2, 4-deacetylneosolaniol, NEO, 9-OH-T-2, and 3′-OH-T-2 had high contents in liver S9 fraction systems, whereas in liver microsomes systems, HT-2, NEO, 9-OH-T-2, and 4-deacetylneosolaniol were the main metabolites.

In summary, a sensitive UPLC-Q/TOF-MS method was applied for the structural elucidation of T-2 toxin metabolites in in vivo and in vitro systems of Wistar rats in this research. Through the combination of the accurate mass measurements providing qualitative information of TOF and the automatic identification function of software Meabolynx^{XS}, in total 19 metabolites of T-2 toxin were detected, and 9 of them were discovered for the first time, such as 15-deacetyl-T-2, 3′-OH-15-deacetyl-T-2, 3′,7-dihydroxy-T-2, isomer of 3′,7-dihydroxy-T-2, 7-OH-HT-2, isomer of 7-OH-HT-2, de-epoxy-3′,7-dihydroxy-HT-2, 9-OH-T-2 and 3′,9-dihydroxy-T-2. In addition, this research demonstrated one novel metabolic pathway of T-2 toxin, hydroxylation at the C-9 position. Furthermore, numerous metabolites of hydroxylation at C-7 of T-2 toxin were detected first in male Wistar rats, showing that hydroxylation at C-7 could also occur in the rodents. Interestingly, there are no metabolites of hydroxylation at C-7 detected in vivo for female rats yet. Furthermore, hydroxylation at C-9 of T-2 toxin was found in in vitro systems, but hydroxylation at C-7 was not. The above results provide an important basis for further study of the toxicological safety evaluation of T-2 toxin.

AUTHOR INFORMATION

Corresponding Author

*(S.Z.) Phone: +86-10-6273-1201. Fax:+86-10-6273-1032. E-mail: suxia@cau.edu.cn.

Author Contributions

‖S.Y. and Y.L. contributed equally to this work.

Funding

The work was supported financially by the National Basic Research Program of China (Grant 2009CB118801) and the International Science and Technology Cooperation Program of China (2012DFG31840). Additionally, D.H. was supported by the National Institute of Environmental Health Sciences (P42ES013661).

Notes

The authors declare no competing financial interest.

ACKNOWLEDGMENTS

We acknowledge Peisheng Feng, Linxia Li, Haixia Wu, Kaili Liu, Tiejun Mi, and Lu Zhang for their timely help in this study.

REFERENCES

(1) Li, Y.; Wang, Z.; Beier, R. C.; Shen, J.; De Smet, D.; De Saeger, S.; Zhang, S. T-2 toxin, a trichothecene mycotoxin: review of toxicity, metabolism, and analytical methods. *J. Agric. Food Chem.* **2011**, *59*, 3441−3453.

(2) Gutleb, A. C.; Morrison, E.; Murk, A. J. Cytotoxicity assays for mycotoxins produced by *Fusarium* strains: a review. *Environ. Toxicol. Pharmacol.* **2002**, *11*, 309−320.

(3) Weidner, M.; Welsch, T.; Hubner, F.; Schwerdt, G.; Gekle, M.; Humpf, H. U. Identification and apoptotic potential of T-2 toxin metabolites in human cells. *J. Agric. Food Chem.* **2012**, *60*, 5676−5684.

(4) Islam, Z.; Nagase, M.; Yoshizawa, T.; Yamauchi, K.; Sakato, N. T-2 toxin induces thymic apoptosis in vivo in mice. *Toxicol. Appl. Pharmacol.* **1998**, *148*, 205−214.

(5) Hymery, N.; Sibiril, Y.; Parent-Massin, D. Improvement of human dendritic cell culture for immunotoxicological investigations. *Cell Biol. Toxicol.* **2006**, *22*, 243−255.

(6) Minervini, F.; Fornelli, F.; Lucivero, G.; Romano, C.; Visconti, A. T-2 toxin immunotoxicity on human B and T lymphoid cell lines. *Toxicology* **2005**, *210*, 81−91.

(7) Wu, J.; Jing, L.; Yuan, H.; Peng, S. Q. T-2 toxin induces apoptosis in ovarian granulosa cells of rats through reactive oxygen species-mediated mitochondrial pathway. *Toxicol. Lett.* **2011**, *202*, 168−177.

(8) Yang, J. Y.; Zhang, Y. F.; Liang, A. M.; Kong, X. F.; Li, Y. X.; Ma, K. W.; Jing, A. H.; Feng, S. Y.; Qiao, X. L. Toxic effects of T-2 toxin on reproductive system in male mice. *Toxicol. Ind. Health* **2010**, *26*, 25−31.

(9) Caloni, F.; Cortinovis, C. Effects of fusariotoxins in the equine species. *Vet. J.* **2010**, *186*, 157−161.

(10) Thompson, W. L.; Wannemacher, R. W., Jr. In vivo effects of T-2 mycotoxin on synthesis of proteins and DNA in rat tissues. *Toxicol. Appl. Pharmacol.* **1990**, *105*, 483−491.

(11) Wu, Q.; Dohnal, V.; Huang, L.; Kuca, K.; Yuan, Z. Metabolic pathways of trichothecenes. *Drug Metab. Rev.* **2010**, *42*, 250−267.

(12) Bennett, J. W.; Klich, M. Mycotoxins. *Clin. Microbiol. Rev.* **2003**, *16*, 497−516.

(13) Velazco, V.; Faifer, G. C.; Godoy, H. M. Differential effects of T-2 toxin on bone marrow and spleen erythropoiesis in mice. *Food Chem. Toxicol.: Int. J.* **1996**, *34*, 371−375.
(14) EFSA Panel on Contaminants in the Food Chain (CONTAM). Scientific Opinion on the risks for animal and public health related to the presence of T-2 and HT-2 toxin in food and feed. *EFSA J.* **2011**, *9*, 2481.
(15) Adejumo, T. O.; Hettwer, U.; Karlovsky, P. Occurrence of *Fusarium* species and trichothecenes in Nigerian maize. *Int. J. Food Microbiol.* **2007**, *116*, 350−357.
(16) Schollenberger, M.; Muller, H. M.; Rufle, M.; Suchy, S.; Plank, S.; Drochner, W. Natural occurrence of 16 fusarium toxins in grains and feedstuffs of plant origin from Germany. *Mycopathologia* **2006**, *161*, 43−52.
(17) Omurtag, G. Z.; Yazicioglu, D. Occurrence of T-2 toxin in processed cereals and pulses in Turkey determined by HPLC and TLC. *Food Addit. Contam.* **2001**, *18*, 844−849.
(18) Ohta, M.; Ishii, K.; Ueno, Y. Metabolism of trichothecene mycotoxins. I. Microsomal deacetylation of T-2 toxin in animal tissues. *J. Biochem.* **1977**, *82*, 1591−1598.
(19) Ellison, R. A.; Kotsonis, F. N. In vitro metabolism of T-2 toxin. *Appl. Microbiol.* **1974**, *27*, 423−424.
(20) Yoshizawa, T.; Swanson, S. P.; Mirocha, C. J. T-2 metabolites in the excreta of broiler chickens administered ^{3}H-labeled T-2 toxin. *Appl. Environ. Microbiol.* **1980**, *39*, 1172−1177.
(21) Visconti, A.; Mirocha, C. J. Identification of various T-2 toxin metabolites in chicken excreta and tissues. *Appl. Environ. Microbiol.* **1985**, *49*, 1246−1250.
(22) Yoshizawa, T.; Swanson, S. P.; Mirocha, C. J. In vitro metabolism of T-2 toxin in rats. *Appl. Environ. Microbiol.* **1980**, *40*, 901−906.
(23) Yoshizawa, T.; Mirocha, C. J.; Behrens, J. C.; Swanson, S. P. Metabolic fate of T-2 toxin in a lactating cow. *Food Cosmet. Toxicol.* **1981**, *19*, 31−39.
(24) Yoshizawa, T.; Sakamoto, T.; Okamoto, K. In vitro formation of 3′-hydroxy T-2 and 3′-hydroxy HT-2 toxins from T-2 toxin by liver homogenates from mice and monkeys. *Appl. Environ. Microbiol.* **1984**, *47*, 130−134.
(25) Visconti, A.; Treeful, L. M.; Mirocha, C. J. Identification of iso-TC-1 as a new T-2 toxin metabolite in cow urine. *Biomed. Mass Spectrom.* **1985**, *12*, 689−694.
(26) Yoshizawa, T.; Sakamoto, T.; Kuwamura, K. Structures of deepoxytrichothecene metabolites from 3′-hydroxy HT-2 toxin and T-2 tetraol in rats. *Appl. Environ. Microbiol.* **1985**, *50*, 676−679.
(27) Kajal Chatterjee, A. V.; Mirocha, C. J. Deepoxy T-2 tetraol: a metabolite of T-2 toxin found in cow urine. *J. Agric. Food Chem.* **1986**, *34*, 695−697.
(28) Swanson, S. P.; Nicoletti, J.; Rood, H. D., Jr.; Buck, W. B.; Cote, L. M.; Yoshizawa, T. Metabolism of three trichothecene mycotoxins, T-2 toxin, diacetoxyscirpenol and deoxynivalenol, by bovine rumen microorganisms. *J. Chromatogr.* **1987**, *414*, 335−342.
(29) Richard, A.; Corley, S. P. S.; William, B. Glucuronide conjugates of T-2 toxin and metabolites in swine bile and urine. *J. Agric. Food Chem.* **1985**, *33*, 1085−1089.
(30) Welsch, T.; Humpf, H. U. HT-2 toxin 4-glucuronide as new T-2 toxin metabolite: enzymatic synthesis, analysis, and species specific formation of T-2 and HT-2 toxin glucuronides by rat, mouse, pig, and human liver microsomes. *J. Agric. Food Chem.* **2012**, *60*, 10170−10178.
(31) Wu, Q.; Engemann, A.; Cramer, B.; Welsch, T.; Yuan, Z. Intestinal metabolism of T-2 toxin in the pig cecum model. *Mycotoxin Res.* **2012**, *28*, 191−198.
(32) Wu, Q.; Huang, L.; Liu, Z.; Yao, M.; Wang, Y.; Dai, M.; Yuan, Z. A comparison of hepatic in vitro metabolism of T-2 toxin in rats, pigs, chickens, and carp. *Xenobiotica; Fate Foreign Compds. Biol. Syst.* **2011**, *41*, 863−873.
(33) Tolonen, A.; Turpeinen, M.; Pelkonen, O. Liquid chromatography-mass spectrometry in in vitro drug metabolite screening. *Drug Discov. Today* **2009**, *14*, 120−133.
(34) Wu, H.; Li, L.; Shen, J.; Wang, Y.; Liu, K.; Zhang, S. In vitro metabolism of cyadox in rat, chicken and swine using ultra-performance liquid chromatography quadrupole time-of-flight mass spectrometry. *J. Pharm. Biomed. Anal.* **2012**, *67−68*, 175−185.
(35) Lowry, O. H.; Rosebrough, N. J.; Farr, A. L.; Randall, R. J. Protein measurement with the Folin phenol reagent. *J. Biol. Chem.* **1951**, *193*, 265−275.